JOURNAL OF THERMOPHYSICS AND HEAT TRANSFER
Vol. 10, No. 1, January–March 1996

Thermal Contact Conductance of Refractory Ceramic Coatings

E. E. Marotta* and L. S. Fletcher†
Texas A&M University, College Station, Texas 77843-3123

The reliability of high-density circuit devices may be improved by enhancing the thermal contact conductance at electronic component interfaces. Previous studies involved metallic coatings, anodized coatings, or bulk ceramic materials between electronic components. This study examines the thermal contact conductance of four ceramic coatings, silicon nitride, boron nitride, aluminum nitride, and titanium nitride (TiN) deposited on aluminum 6101-T6 and TiN deposited on copper C11000-H03. The thermal contact conductance of beryllium oxide (BeO) deposited on aluminum 6101-T6 was also experimentally measured. Three of the coatings showed two orders of magnitude improvement when compared to an anodized layer. Experimental thermal conductance values for TiN deposited on copper showed four times the improvement over a nickel-plated coating. A comparison of the coatings to an aluminum 6101-T6 surface in contact with aluminum A356-61 indicates that the titanium nitride coatings have the highest thermal contact conductance and that the coatings only significantly deviate from the bare aluminum case at the higher pressures (greater than 344 kPa). Experimental thermal conductance values for BeO deposited on aluminum 6101-T6 ranged from 1308.7 to 25,688.7 W/m²-K, whereas thermal conductance values for TiN deposited on aluminum 6101-T6 in contact with electroplated silver deposited on aluminum A356-T61 varied from 1169.4 to 13,152.1 W/m²-K for the range of parameters tested. The results predicted by the Antonetti and Yovanovich model lie well above the experimental values obtained for both bare surfaces and for several ceramic coatings (titanium nitride and beryllium oxide coatings deposited on aluminum 6101-T6 were the only exception). The thermal contact conductance values for the ceramic and oxide coatings were compared to the predicted results from Yip's model that lie well below the measured values; indicating higher thermal contact conductance.

Nomenclature

F = flatness
H = hardness
h = thermal conductance
$h_{c,0}$ = thermal conductance between the substrate and coating
$h_{c,1}$ = thermal conductance between the uncoated substrate and coating
h_t = total conductance
k = thermal conductivity
R = roughness
R_b = bulk coating resistance
$R_{c,1}$ = contact resistance, interface 1
$R_{c,2}$ = contact resistance, interface 2
R_t = total resistance
S = asperity slope
t = coating thickness
W = waviness

Subscripts
a = average
c = coated
eff = effective
q = root mean square
s = substrate
u = uncoated

Presented as Paper 93-2777 at the AIAA 28th Thermophysics Conference, Orlando, FL, July 6–9, 1993; received April 4, 1995; revision received April 16, 1995; accepted for publication July 20, 1995.

*Graduate Research Assistant, Mechanical Engineering Department. Student Member AIAA.

†Thomas A. Dietz Professor, Mechanical Engineering Department. Fellow AIAA.

Introduction

As circuit densities increase to achieve the system performances required by today's scientific and engineering communities, the need to improve system reliability becomes paramount. The reliability of electronic components and systems is directly related to system operating temperatures. Cooling schemes have been developed that will maintain device temperatures within their optimum design specifications, however, other techniques for maintaining or reducing operating temperatures must be explored.

One factor that can contribute to the removal of heat from microelectronic devices is an increase in the thermal contact conductance at component junctions. The choice of interstitial material coating or film for a particular microelectronic device application is governed by such factors as contact pressure and temperature, environmental conditions, and the degree to which it is desired to reduce or enhance heat flow across the junction. Various thermal control materials are available and these can be classified by their compositions as greases and oils, metallic foils and screens, composites and cements, and surface treatments.[1]

Marotta et al.[2] conducted a comprehensive review of the literature for nonmetallic materials suitable for interface coating. The review considered four groups of nonmetallic materials as possible candidates for enhancement of the thermal contact conductance for electronic module packaging. These four nonmetallic material groups are classified as 1) oxide-, 2) carbon-, 3) ceramic-, and 4) polymer-based materials. The results of this evaluation suggest that oxide films must remain relatively thin with a hardness less than the substrate for any beneficial enhancement of the contact conductance. Carbon-based coatings such as polycrystalline and diamond-like carbon films offer excellent thermophysical properties that make them attractive as coatings. Ceramics, such as titanium nitride (TiN), silicon carbide (SiC), titanium carbide (TiC), and aluminum nitride (AlN) have shown suitable thermal and mechanical properties with a wide range of applications, however, these materials serve primarily as thermal barriers rather than thermal enhancement materials.

Majumdar[3] conducted an experimental investigation of the effect of surface deformation on thermal contact conductance for a metal–ceramic interface of aluminum nitride in contact with both aluminum and copper with smooth surface profiles [$\delta = 0.50\ \mu$m (19.7 μin.)]. His experiments showed that the deformations could be predominantly elastic. He concluded that surface asperities that deform plastically do so only for the first loading, while subsequent loading and unloading led to predominantly elastic deformations. For a load range between 1.6×10^4–1.6×10^5 N/m^2 (2.3–23 psi), which are pressures comparable to those used in electronic packaging, the experiments indicated a plastic deformation of the aluminum metal since the data showed a hysteresis effect. However, measurements for the copper and aluminum nitride junction showed no hysteresis, thus indicating predominantly elastic deformation.

Fletcher and Sparks[4] conducted an experimental investigation to determine the overall thermal conductance, the thermal contact conductance, and thermal conductivity of selected porous ceramic materials. The authors concluded that the overall thermal conductance increased with increasing temperature and porosity; thus, they conclude that the use of porous ceramics will depend upon other properties rather than the thermal characteristics since this characteristic was similar for all the ceramic materials.

Sheffield and Chung[5] conducted an experimental investigation to measure the thermal contact conductance between metal and ceramic substrate junctions. Because metallic oxides have a low coefficient of thermal expansion and high-temperature stability, aluminum oxide samples were coated with thin coatings of copper or aluminum and experimental measurements were made for two different surface roughnesses. Their experimental data showed that the copper-coated aluminum oxide samples had a thermal contact conductance enhancement of 44 and 58%, respectively, for the smooth and rough surface. However, the aluminum-coated aluminum oxide samples had a reduction in enhancement by approximately 25 and 28%, respectively, for each surface roughness.

When two surfaces have a thin coating of material between them, the overall joint resistance can be expressed as the summation of the two thermal contact resistances and the bulk resistance of the interfacial coating material as described by Peterson and Fletcher[6]:

$$R_t = R_{c,1} + R_b + R_{c,2} \tag{1}$$

when expressed in terms of thermal conductances

$$(1/h_t) = (1/h_{c,0}) + (1/h_b) + (1/h_{c,1}) \tag{2}$$

Because of interdiffusional bonding of molecules between the coating and the copper or aluminum substrate surface, $h_{c,0}$ can be considered to be negligible. The expression reduces to the summation of the thermal contact conductance and the bulk resistance:

$$(1/h_t) = -(1/h_{c,1}) + (1/h_b) \tag{3}$$

The bulk conductance can be expressed as a function of the thermal conductivity and material thickness, thus, the effective thermal conductivity of the coating material can be expressed as

$$k_{\text{eff}} = \frac{t}{[(1/h_t) - (1/h_{c,1})]} \tag{4}$$

Both the contact conductance between the ceramic coating and prime surface and the thermal conductivity of the ceramic coating may be determined using the results of several different thickness coatings. This experimental study will make use of Eq. (3) to calculate the overall joint thermal conductance.

Ceramic coatings can be applied by techniques that give rise to their physical and thermal properties. These processes include plasma/flame spraying and physical vapor deposition (PVD) refractory deposition. Plasma/flame sprayed coatings have found wide acceptance as both protective and decorative coatings. Ceramic flame-sprayed coatings include the oxides, borides, nitrides, and silicides, as well as a number of glass compositions. These ceramic coatings have been used for thermal insulation, electrical insulation, and erosion and corrosion resistance.

Refractory coatings, such as TiC, TiN, SiC, AlN, boron nitride (BN), and Si_3N_4 can be used to provide wear-resistance and corrosion-protection for different environmental conditions. PVD is an important technique for deposition of these refractory compounds. One of the beneficial effects of the high temperatures used in PVD is that the bond strength between the coatings and the substrate material is very high. Both the coating and the material form transition zones by interdiffusion. Cemented carbide steels, when coated with TiN, can form intermediate layers of TiC and titanium carbonitride (Ti-CN), which greatly enhance the bond strength between coating and substrate.

Refractory coatings deposited by a PVD method have found widespread acceptance for the protection of bearings, forming tools, and cutting inserts. Their mechanical properties and chemical stability are also finding use in the microelectronic industry where protective coatings are essential for electronic packaging of high-power chips. These coatings are explored as possible candidates for the improvement of the interface thermal enhancement between component interfaces. This article describes the results of an experimental investigation to determine the thermal contact conductance of several refractory ceramic coatings deposited onto aluminum 6101-T6 and copper C11000-H03 in contact with bare aluminum A356-T61.

Experimental Program

The experimental investigation was conducted in a manner similar to previously reported investigations.[4,7–9] The facility, ceramic material selection, and procedure are described in this section. The experimental test facility consisted of a vertical column consisting of a frame with sliding plates for supporting two combination heat source/sink specimen holder assemblies, the test samples, a load cell, and pneumatic bellows. The axial force on the test column was applied by pres-

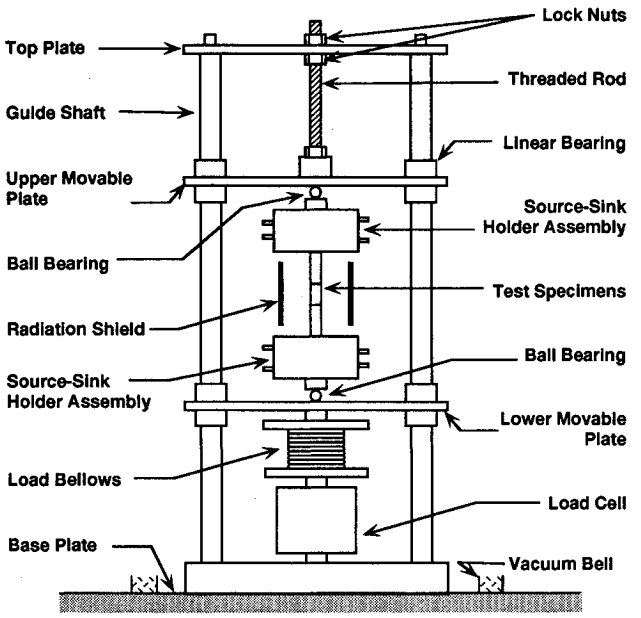

Fig. 1 Experimental apparatus.

surizing the bellows and the contact load was monitored by a load cell and signal amplifier. Uniform contact pressure over the test interfaces was assured by the use of two hardened stainless steel balls that transfer load from the frame to the source-sink-holder assemblies and, in turn, the specimens. Flexible neoprene hoses were used to supply coolant to the holder assemblies in order to essentially eliminate lateral loads that would skew the pressure distribution over the interfaces.

The experimental facility was housed in a vacuum environment at a pressure of 1.4×10^{-1} Pa (1×10^{-5} torr), which was maintained by a Varian VHS-6 oil diffusion pump backed by an Alcatel 2300 two-stage rotary pump. The vacuum pressure was monitored by thermocouple and filament gauges connected to a Perkin Elmer Monitor 300 indicator. Figure 1 shows a schematic of the experimental facility.

Test Specimens

The thermal contact conductance specimens were each 2.54 cm (1.00 in.) in diameter. The upper and lower specimens were 10.16 cm (4.00 in.) long and were fabricated from aluminum alloy A356-T61, whereas the middle specimen is 3.81 cm (1.50 in.) long and was machined from aluminum alloy 6101-T6 or copper C11000-H03. The aluminum 6101-T6 and copper C11000-H03 specimens were coated as described in the next section.

Each of the three samples were instrumented with five special limit of error (1.1°C) K type thermocouples (AWG 30) inserted into 0.12-cm- (0.047-in.-) diam holes drilled radially to the specimen axes at 0.635-cm (0.25-in.) intervals. Aluminum powder was then tamped into the holes to ensure good thermal contact of the thermocouple beads to the side of the holes. The thermocouples were connected to a Hewlett Packard 3497A data acquisition unit.

Physical Vapor Deposition

The process used for depositing TiN onto copper C11000-H03 involved the sputtering of a solid TiN compound target onto the negatively biased substrate set between 100–2000 V, substrate temperatures between 200–550°C (392–1022°F), substrate current density between 2–5 A, and substrate heating and surface precleaning (on an atomic level) using argon ions. Titanium nitride film thicknesses between 1–5 μm (39.4–196.8 μin.) were deposited using these process parameters. Deposition rates of less than 0.2 μm/min were obtained with these parameters. Similar deposition parameters were used to deposit beryllium oxide (BeO) coatings on aluminum 6101-T6 substrates.

Boron nitride (BN) and aluminum nitride (AlN) ceramic films were deposited in a rf magnetron (13.56 MHz) sputtering system equipped with a 2000 l/s cryogenic pumping system. Ultimate pressure achievable with the stainless steel vacuum system is less than 7×10^{-5} Pa (5×10^{-7} torr) as measured by an ionization-type gauge while the deposition pressure was maintained at less than 1×10^{-3} Pa (8×10^{-6} torr) as measured with a capacitive manometer gauge. The rf magnetron targets were fabricated from 99.99% pure boron nitride and aluminum nitride material and depositions were carried out in an argon/nitrogen gas mixture. The substrates were plasma etched in a RF plasma prior to depositing the BN and AlN films to completely de-gas and clean the substrate surfaces for contaminates.

Both boron nitride and aluminum nitride depositions (except TiN) were performed in an argon/nitrogen gas mixture of 10:1 with substrates biased between 25–125 V dc to improve adhesion and microstructure during processing. No substrate heating was used, but plasma etching and heating attributable to deposition conditions resulted in a steady-state coating temperature of 232–260°C (450–500°F). With these process parameters, deposition rates of 2 Å/s were achieved for both boron nitride and aluminum nitride films. A similar deposition technique was employed for silicon nitride films deposited on aluminum 6101-T6.

Surface Characteristics

All surfaces were characterized utilizing a Federal Products Surfanalyzer 4000/5000 profilometer. Root mean square and centerline average (CLA) roughness, rms and average waviness, overall flatness deviation, and rms asperity slope infor-

Table 1 Thermal conductivity, Vicker's microhardness, and surface metrological data

Base material contact pair	Coating material	k_s/k_c, W/m K	t, μin.	t, μm	H_u/H_c, kg/mm^2	Ra, μm	R_q, μm	W_a, μm	W_q, μm	F, μm	S_q, rad
A356-T61 F1	Bare	150	0	0	85	0.64	0.83	0.31	0.37	7.15	0.155
A356-T61 F2	Bare	150	0	0	85	0.65	0.84	0.43	0.52	8.15	0.160
Al601-T6	Bare	201	0	0	41.44	0.62	0.80	1.04	1.25	9.35	0.142
Cu C1100-H03	Bare	402	0	0	55.31	0.36	0.45	0.25	0.32	1.66	0.114
Cu C11000-H03	Titanium nitride	402/24	51.18	1.3	55.31/47.50	1.33	1.65	1.68	1.98	7.80	0.250
Bare A356-T61	Deposited on copper		149.61	3.8	55.31/65.00	0.48	0.64	0.95	1.18	4.65	0.184
	C11000-H03		208.66	5.3	55.31/70.00	2.19	2.74	1.36	1.51	5.85	0.359
Al 6101-T6	Titanium nitride	201/24	31.49	0.8	41.44	0.60	0.80	0.80	1.00	3.60	0.200
Bare A356-T61	Deposited on aluminum		139.76	3.55	41.44	0.25	0.38	2.90	3.28	9.75	0.140
	6101-T6		210.63	5.35	41.44/268.00	1.16	1.51	1.12	1.46	6.05	0.220
Al 6101-T6	Boron nitride	201/23	39.37	1	41.44/38.00	0.78	0.97	1.92	2.30	8.55	0.204
Bare A356-T61	Deposited on aluminum		118.11	3	41.44/49.00	0.60	0.77	0.48	0.68	3.15	0.162
	6101-T6		216.54	5.5	41.44/49.00	0.90	1.15	1.29	1.56	5.95	0.161
Al 6101-T6-	Aluminum nitride	201/70	39.37	1	41.44/72.00	0.80	1.02	1.70	2.01	7.45	0.221
Bare A356-T61	Deposited on aluminum		118.11	3	41.44/72.00	0.57	0.74	1.06	2.05	5.40	0.156
	6101-T6		196.85	5	41.44/325.00	0.71	0.95	1.43	1.78	6.40	0.180
Al 6101-T6-	Silicon nitride	201/20	39.37	1	41.44	0.39	0.51	2.70	3.37	13.85	0.160
Bare A356-T61	Deposited on aluminum		78.74	2	41.44	0.47	0.60	2.14	2.67	9.95	0.159
	6101-T6		118.11	3	41.44/100.00	0.49	0.66	1.89	2.01	15.60	0.159
Al 6101-T6-	Beryllium oxide	201/270	39.37	1	41.44/75.00	0.76	0.96	1.90	2.29	9.30	0.220
Bare A356-T61	Deposited on aluminum		118.11	3	41.44/500.00	0.77	1.01	1.66	2.02	8.10	0.190
	6101-T6		196.85	5	41.44/500.00	1.32	1.82	8.84	10.44	38.05	0.220
Al 6101-T6-	Titanium nitride	201/24	31.49	0.8	41.44	0.60	0.80	0.80	1.00	3.60	0.200
A356-T61	Deposited on aluminum		139.76	3.55	41.44	0.25	0.38	2.90	3.28	9.75	0.140
	6101-T6		210.63	5.35	41.44/268.00	1.16	1.51	1.12	1.46	6.05	0.220
	Electro-plated silver (Ag)	201/427	2000	50.8	41.44/94.00	1.00	1.30	3.40	3.90	14.20	0.191
	Deposited on aluminum A356-T61										

mation are listed in Table 1. The surface microhardness also subsequently influences the contact conductance values. Consequently, the Vickers microhardness of coupons of each of the six types of coatings, in thicknesses similar to those employed in contact conductance tests, were measured over an indentor load range of 25–1000 g force.

Test Procedure

Successive tests were conducted with ceramic coatings of varying thicknesses. Each test begins with insertion of the selected middle ceramic-coated aluminum 6101-T6 or copper C11000-H03 sample between the upper and lower aluminum A356-T61 fluxmeters. A special alignment fixture is clamped around the column of three specimens to ensure exact coaxial mating of the surfaces. A light load is applied, then the alignment fixture is removed. A preload pressure of 2760 kPa (400 psi) is applied. The bell jar is sealed over the apparatus and a vacuum drawn. Power is supplied to the heater that is located on the source-sink-holder assembly and coolant is pumped through the opposite assembly.

Experimental data were obtained utilizing a Hewlett Packard data-logger, which was controlled by a personal computer via an IEEE-488 bus. The temperature gradients and thermal conductivities of the heat fluxmeters were used to determine the heat fluxes in both the upper and lower fluxmeters. The temperature change across the ceramic coating was determined by extrapolating the thermal gradient in the heat fluxmeters to the junction surface.

The reported contact conductance data are for the case of heat flux passing from the ceramic-coated aluminum 6101-T6 or copper C11000-H03 specimen to the bare aluminum A356 specimen. The experimental investigation was conducted at contact pressures of 172–2760 kPa (25–400 psi) with coating thicknesses ranging from 1.0 to 5.0 μm (0.04 to 0.20 mil). To make an appropriate comparison, tests were conducted at mean interface temperatures of 20, 60, and 100°C (68, 140, and 212°F). The experimental results include the thermal contact conductance for each ceramic coating thickness over the range of pressures and temperatures investigated.

Data Analysis

Once the test column temperature profile achieved a quasi-steady-state condition, which is assumed to have occurred when the mean thermal contact conductance changes by no more than 0.5%/h, a data acquisition and analysis program is executed. The temperature gradient in each sample, computed from a linear least-squares regression of the individual thermocouple readings, and its temperature-dependent conductivity, obtained from a prior calibration, are used to calculate the heat flux through each specimen. The temperature profiles in the specimens are extrapolated to the interface to obtain the temperature discontinuity across the interface. The contact conductance is computed as the quotient of the mean heat flux across the junction and the temperature discontinuity.

Uncertainty Analysis

Experimental uncertainties in contact conductance data arise from a number of sources, the most predominant of which is the randomness in thermocouple readings due to slight variations in their composition. Uncertainties in the specimen thermal conductivities are 2.5% for the aluminum A356-T61, 2.8% for the aluminum 6101-T6 and 4.2% for the copper C11000-H03. The analysis method of Kline and McClintock[10] yields an average overall uncertainty of 7.2% for the thermal contact conductance of TiN, 10.4% for boron nitride, 9.9% for aluminum nitride, 10.0% for silicon nitride, and 10.4% for beryllium oxide-coated aluminum 6101-T6 to bare aluminum A356-T61. The overall uncertainty for the thermal contact conductance of titanium nitride-coated copper C11000-H03 to bare aluminum A356-T61 was 12.2%, whereas the uncertainty for titanium nitride-coated aluminum 6101-T6 to silver-coated aluminum A356-T61 was 12.2%.

Results and Discussion

Ceramics, in contrast to metals, generally exhibit better structural and thermal capabilities at high temperatures. In general, ceramics are more resistant to creep, oxidation, corrosion, erosion, and wear, as well as being better thermal insulators.

Thermal Contact Conductance

The thermal contact conductance for titanium nitride coatings deposited on copper C11000-H03 in contact with bare aluminum A356-T61 is shown in Fig. 2. Three different coating thicknesses were tested to determine the trend in thermal contact conductance with varying layer thickness. For titanium nitride-coated copper C11000-H03 in contact with bare aluminum A356-T61, the thermal contact conductance varies from 2500 to 28,000 W/m^2-K (429 to 4803.9 Btu/h ft^2 °F). Figure 2 clearly shows an increase in thermal contact conductance with increasing interface pressure and interface temperature. Surprisingly, the titanium nitride coating thickness of 3.8 μm (149 μin.) had the overall highest thermal contact conductance of the three coating thicknesses for all three interface temperatures. This result can be attributed to the lower coating surface roughness [R_a = 0.48 μm (18.89 μin.)] when compared to both the thinner coating [R_a = 1.33 μm (52.36 μin.)] and the heavier coating layer [R_a = 2.19 μm (86.22 μin.)]. The variation in surface roughness for each layer can only be a direct result of the deposition process since all surfaces, prior to TiN processing, which were measured indicated almost identical surface roughness.

The thermal contact conductance of bare aluminum A356-T61 in contact with nickel-plated copper C11000-H03 is also shown in Fig. 2. The thermal contact conductance for the three TiN layers, at each interface temperature, is compared to a nickel-plated coating with a thickness of 41.3 μm (1625.9 μin.). The thermal contact conductance values for TiN coatings show a factor of 4 improvement over the nickel-plated coating, but this can be attributed to the lower TiN layer thickness and less bulk resistance.

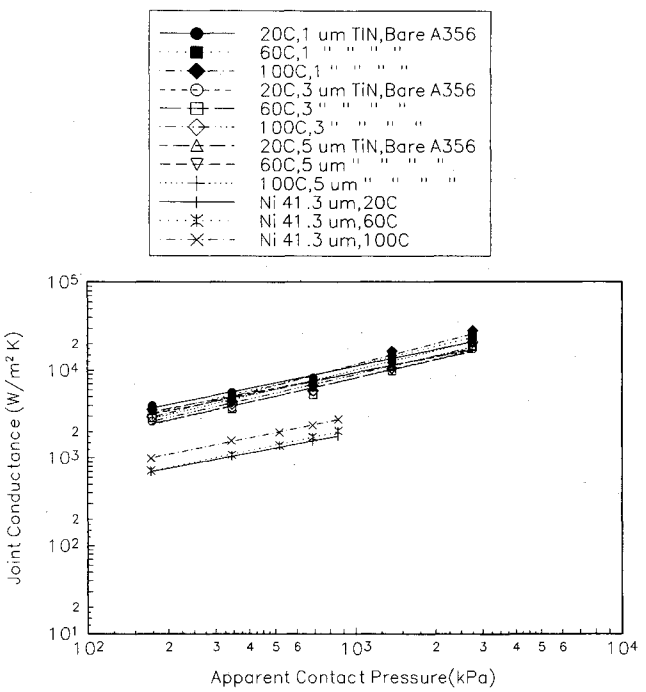

Fig. 2 Thermal contact conductance of titanium nitride on copper C11000-H03 in contact with bare aluminum A356-T61.

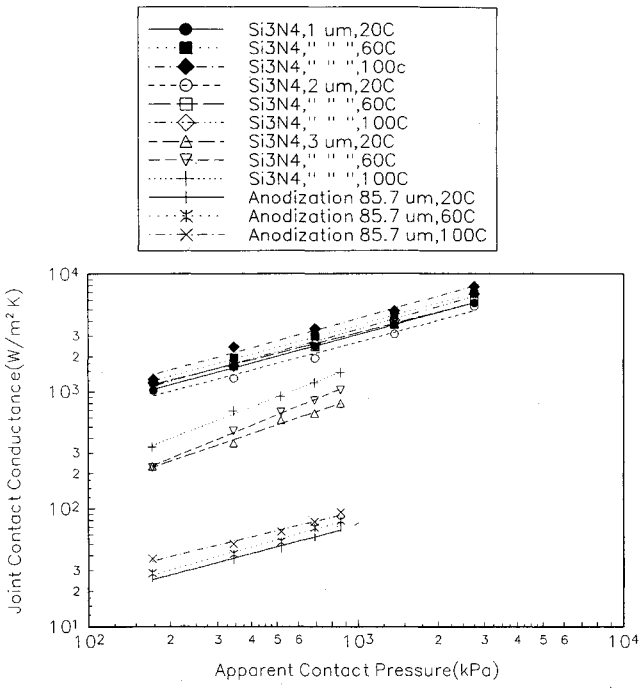

Fig. 3 Thermal contact conductance of silicon nitride on aluminum 6101-T6 in contact with bare aluminum A356-T61.

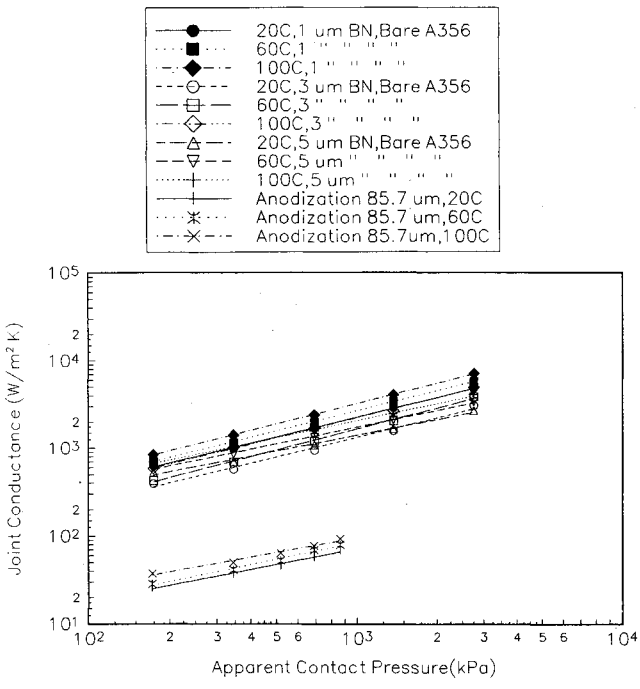

Fig. 4 Thermal contact conductance of boron nitride on aluminum 6101-T6 in contact with bare aluminum A356-T61.

The thermal contact conductance for silicon nitride-coated aluminum 6101-T6 for thicknesses in the range of 1–3 μm (39.7–118.9 μin.) is presented in Fig. 3. For silicon nitride deposited on aluminum 6101-T6 to bare A356, the thermal contact conductance varies from 204.0 to 8500 W/m²-K (35 to 1464.8 Btu/h ft² °F). The thermal contact conductance increases with increasing interface pressure and temperature and decreases with increase in coating thickness.

The thermal contact conductance for silicon nitride-coated aluminum 6101-T6 is also compared to an anodized film grown to a thickness of 85.7 μm (3370 μin.), which is presently used for standard electronic module (SEM) coatings. Two orders of magnitude increase in thermal contact conductance values is observed for the silicon nitride layer over that of the anodized coating. As with the titanium nitride layers, the large difference between the two coatings can be explained by the lower coating thicknesses employed for the silicon nitride. An extensive study of the effect on thermal contact conductance values for several anodizing electrolytes and coating thicknesses was conducted by Lambert et al.[11]

The thermal contact conductance of boron nitride deposited on aluminum 6101-T6 and a comparison to an anodized coating is shown in Fig. 4. The thermal contact conductance values are shown as a function of increasing pressure and temperature. The thermal contact conductance varied from 400 to 7500 W/m²-K (68 to 1286.76 Btu/h ft²°F) for the range of parameters tested. The thermal contact conductance also increased two orders of magnitude when compared to the thermal contact conductance of the anodized coating. The general trend was for increasing thermal contact conductance with increasing interface pressure and temperature, with higher values for thinner coatings. There is little variation in conductance for boron nitride thicknesses of 3–5 μm, however, the difference for a 1-μm coating thickness can be easily seen.

The thermal contact conductance for varying thicknesses of aluminum nitride (AlN) deposited on aluminum 6101-T6 in contact with uncoated aluminum A356-T61 is shown by Fig. 5. The thermal contact conductance varied from 1100 to 15,000 W/m²-K (187.0 to 2550.0 Btu/h ft² °F) for the range of parameters tested, with the highest values obtained for the 1-μm layer thickness. The thermal contact conductance values for both the 3- and 5-μm layers were almost indistinguishable from each other for the parameters tested.

Figure 5 also includes a comparison of the thermal contact conductance for all three layer thicknesses with values obtained for an anodized layer. As with previous plots, the thermal contact conductance values for TiN were two orders of magnitude higher than the anodized film.

The thermal contact conductance of titanium nitride deposited on aluminum 6101-T6 in contact with bare aluminum A356-T61 is shown in Fig. 6. The thermal contact conductance varied from 1745 to 30,000 W/m²-K (307.17 to 5283.55 Btu/ft² h °F) for the range of parameters tested, with the highest

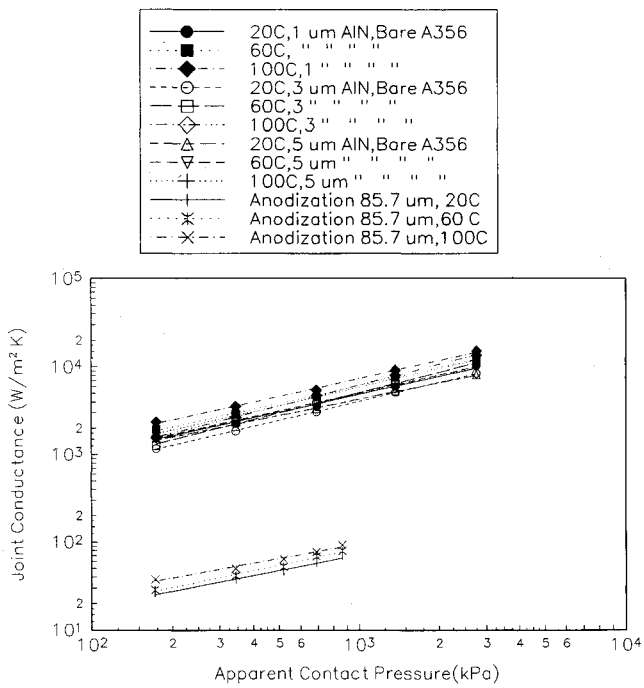

Fig. 5 Thermal contact conductance of aluminum nitride on aluminum 6101-T6 in contact with bare aluminum A356-T61.

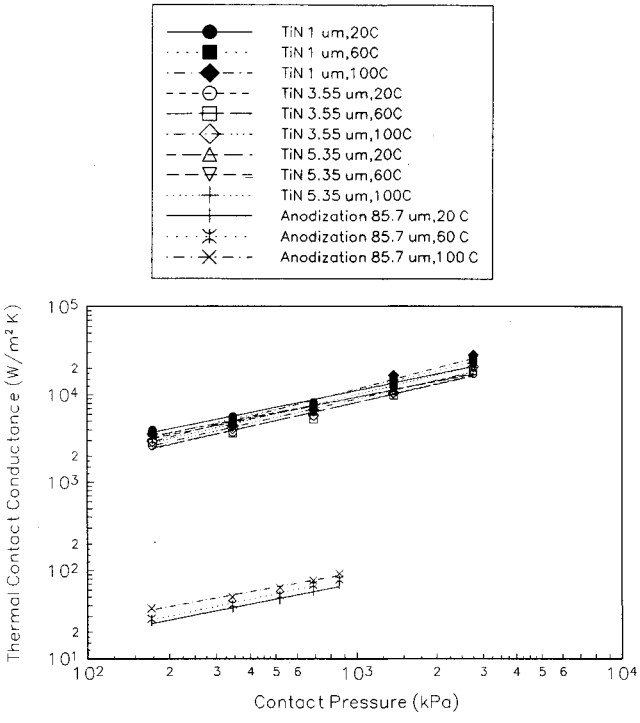

Fig. 6 Thermal contact conductance of titanium nitride on aluminum 6101-T6 in contact with bare aluminum A356-T61.

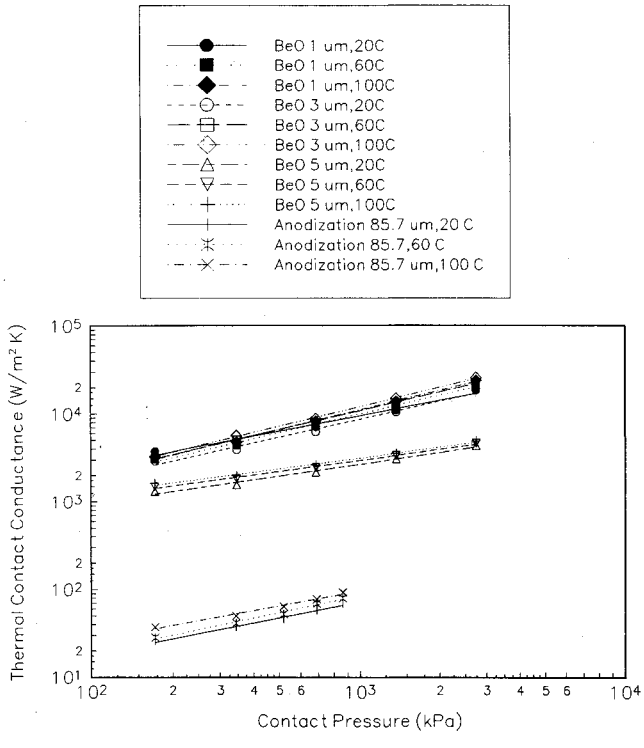

Fig. 7 Thermal contact conductance of beryllium oxide on aluminum 6101-T6 in contact with bare aluminum A356-T61.

values obtained from the 1-μm coating thickness. These coatings had the highest thermal contact conductance values for the refractory ceramic group and greater than aluminum nitride by a factor of 1.5–2.0 for the range of test parameters conducted. The thermal contact conductance values for the 3- and 5-μm (118.9- and 196.8-μin.) coatings had slight variations, but were lower for the 1-μm (39.37-μin.) coating thickness. The thermal contact conductance values for TiN coatings showed very good results for the copper C11000-H03 specimens (values were 16.0% higher than TiN on aluminum 6101-T6 for similar coating thickness), thus, TiN appears to be a good coating for both metallic materials.

The thermal contact conductance of beryllium oxide deposited on aluminum 6101-T6 is shown in Fig. 7. The thermal contact conductance ranged from 1308 to 24,000 W/m²-K (230.36 to 4226.80 Btu/ft² h °F) for the range of parameters tested. The 1- and 3-μm (39.37- and 118.9-μin.) coatings had the highest thermal contact conductance with slight deviations between the two coating thicknesses. However, there was a substantial decrease in thermal conductance for the 5-μm coating thickness when compared to the two thinner coatings. This drop in thermal conductance values can be attributed to the increase of the specimen out of flatness by a factor of three [9 vs 38 μm (354 vs 1496 μin.)] when compared to the other two specimens, however, this flatness measurement is within the applied specification of 50.4 μm (0.002 in.).

Thermal Conductance Comparison

A comparison of the thermal contact conductance, at an interface temperature of 60°C, of five refractory ceramics and two diamond-like carbon coatings with varying thicknesses deposited on aluminum 6101-T6 in contact with a bare aluminum 6101-T6 thermal surface is shown in Figs. 8–10. A comparison of the thermal contact conductance for each coating thickness indicates that the 1-μm (39.37-μin.) titanium nitride coating thickness has the highest overall thermal contact conductance values for the range of parameters tested. Beryllium oxide (BeO) was below the titanium nitride coating followed by aluminum nitride, silicon nitride, and boron nitride coatings. In Fig. 9, the thermal contact conductance for the 3-μm (118.9-μin.) thickness shows no difference between the beryllium oxide and the titanium nitride coatings. The thermal contact conductance for aluminum nitride, boron nitride, and the two diamond-like coatings is well below both the BeO and TiN coatings. In Fig. 10, the 5-μm thickness coatings showed a significant decrease in thermal contact conductance with titanium nitride providing the highest conductance. Also, a very significant decrease in conductance was observed for the BeO coating with no increase in conductance with increasing apparent interface pressure. This

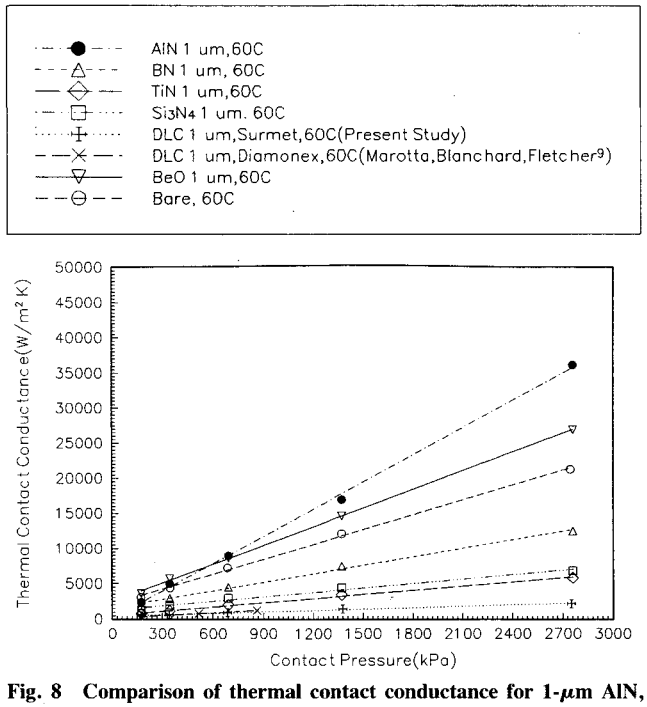

Fig. 8 Comparison of thermal contact conductance for 1-μm AlN, BN, TiN, Si_3N_4, BeO, and DLC on aluminum 6101-T6 in contact with bare aluminum A356-T61.

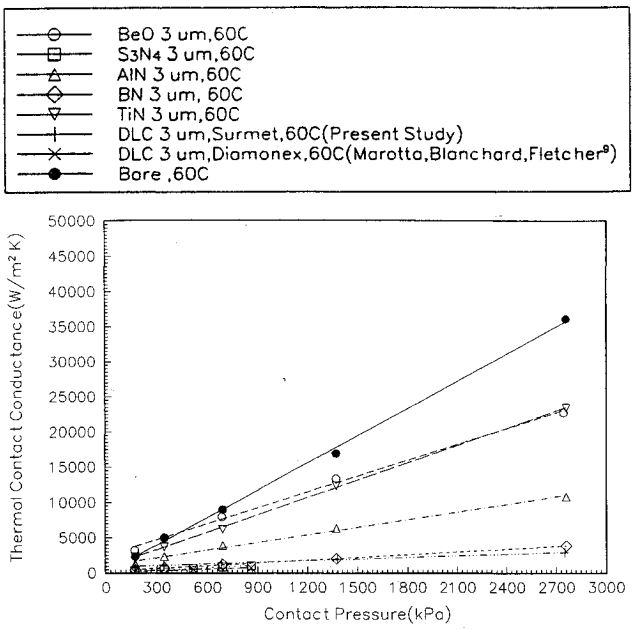

Fig. 9 Comparison of thermal contact conductance for 3-μm AlN, BN, TiN, Si_3N_4, BeO, and DLC on aluminum 6101-T6 in contact with bare aluminum A356-T61.

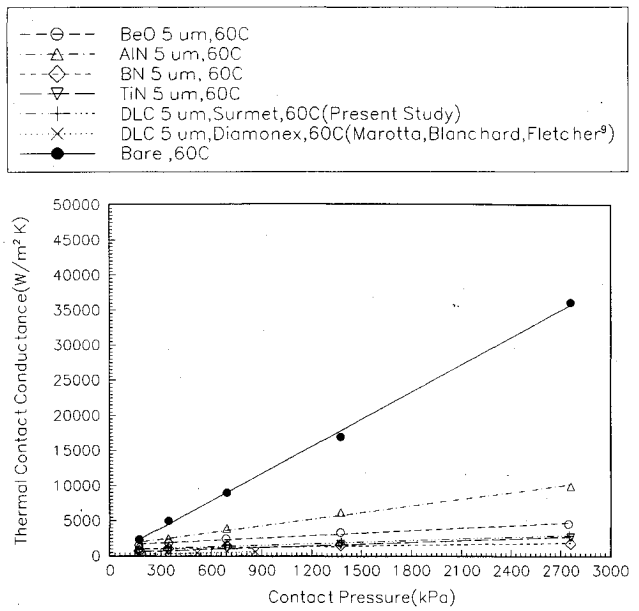

Fig. 10 Comparison of thermal contact conductance for 5-μm AlN, BN, TiN, Si_3N_4, BeO, and DLC on aluminum 6101-T6 in contact with bare aluminum A356-T61.

decrease in conductance for the beryllium oxide coating can be attributed to the difference in flatness for this surface (9 vs 38 μm), resulting in an effective gap between surfaces that was much greater than the other specimens, and caused an increase to the interface resistance. Even with a factor of 3 increase in flatness, this surface still meets the flatness specification of 50.4 μm (0.002 in.). Overall, a titanium nitride coating gives the best thermal conductance from the ceramic group, and beryllium oxide is second.

The thermal contact conductance of titanium nitride deposited on aluminum 6101-T6 in contact with electroplated silver-coated aluminum A356-T61 is shown in Fig. 11. The thermal conductance values varied from 1169.4 to 13,152.1 W/m²-K (205.8 to 2315.15 Btu/ft² h °F) for the range of parameters tested. The thermal contact conductance of vapor-deposited, electroplated, and flame-sprayed silver deposited on aluminum A356-T61 in contact with anodized aluminum 6101-T6 was conducted by Lambert et al.[12] and is presented in Fig. 11 for comparison. The thermal conductance values for the titanium and electroplated silver combination show two orders of magnitude improvement over the anodization and silver coating combinations for the parameters tested. This improvement in thermal contact conductance can be attributed to the thinner coating thicknesses and the higher thermal conductivity of the titanium nitride coating.

Comparison to Antonetti and Yovanovich and Yip Models

The thermal contact conductance values for the thickest coating of each material measured in this study are compared with existing thermomechanical models developed by Antonetti and Yovanovich[13] and Yip.[4] The thermal contact con-

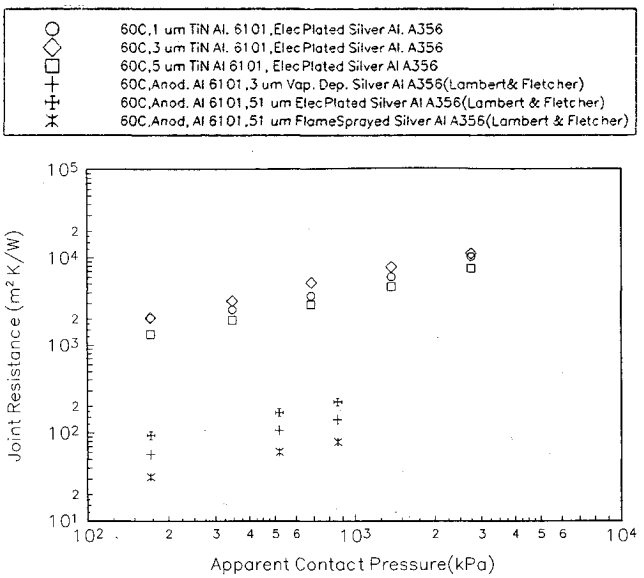

Fig. 11 Comparison of thermal contact conductance for TiN and anodized aluminum 6101-T6 in contact with vapor deposited, electroplated, and flame-sprayed silver on aluminum A356-T61.

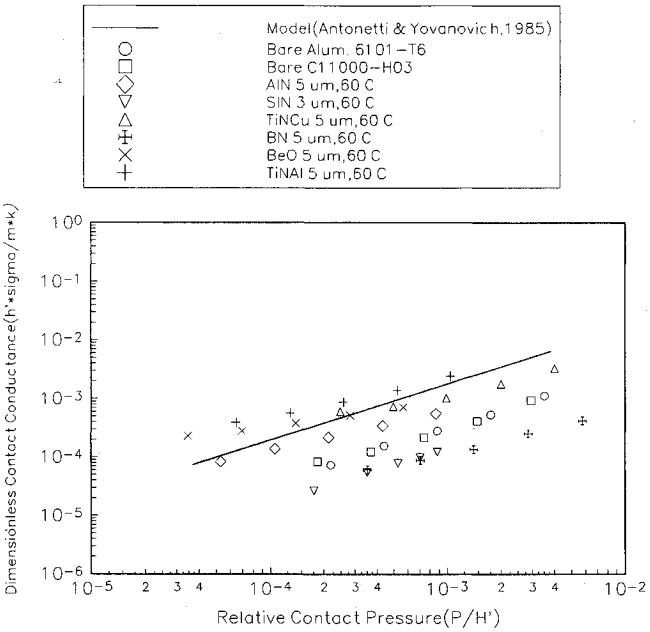

Fig. 12 Comparison of dimensionless thermal contact conductance for AlN, BN, TiN, Si_3N_4, and BeO with model from Antonetti and Yovanovich.[13]

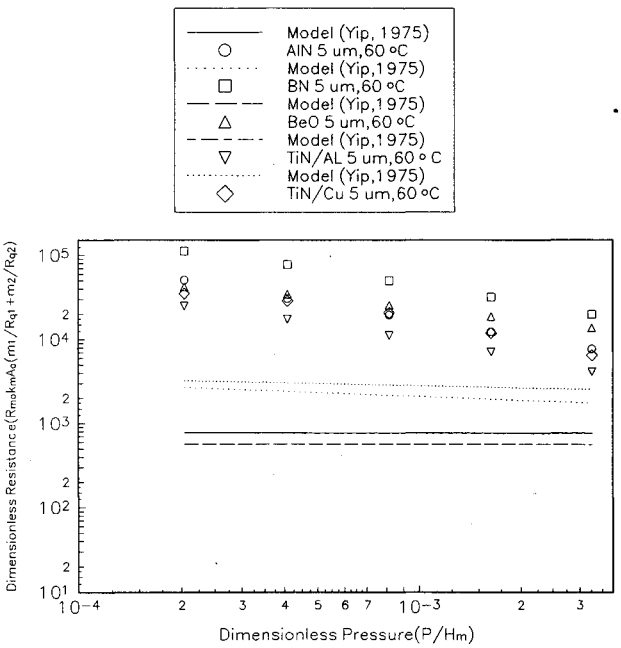

Fig. 13 Comparison of dimensionless thermal contact resistance for AlN, BN, TiN, Si_3N_4, and BeO with model from Yip.[14]

ductance values predicted by Antonetti and Yovanovich are shown in Fig. 12. For both bare metallic surfaces (bare 6101-T6 and C11000-H03) in contact with bare aluminum A356-T61, the predicted values consistently lie above the measured values and also lie above several of the ceramic coatings. Only titanium nitride and beryllium oxide deposited on aluminum 6101-T6 lie along the predictive curve at higher relative pressures, however, the measured values deviate as much as a factor of 3 from the curve for lower relative pressures. The main factors causing the deviation from the model may be the nonflat (nonoptically flat) contacting surfaces at the joint and the lack of precise values for the thermal conductivities of the deposited coatings.

The thermal contact conductance values for the ceramic and oxide coatings measured in this study are compared to Yip's model with the results shown in Fig. 13. The predictive curve for each material type lies well below the measured values, which indicates lower thermal contact resistance for the range of relative pressures tested. Also, the slope of the predictive curves remains relatively flat with decreasing relative pressures while the measured values have an increasing negative slope. The differences between Yip's model and the measured values may be attributed to the nonflatness of the contacting surfaces, which leads to lower real contact surface and lower number of contact spots. The model also does not take into account an effective microhardness of the coating/substrate combination, which may lead to a lower separation distance between the mean line of the oxide or ceramic surface and the interface (greater effective gap at the interface). The basic assumptions made in Yip's model do not apply for the experimentally measured values of thermal resistance at the coated junctions.

Conclusions and Recommendations

Experimental thermal contact conductance measurements were made for four refractory ceramics, including titanium nitride, silicon nitride, boron nitride, and aluminum nitride, deposited on copper C11000-H03 and aluminum 6101-T6 and one oxide material, such as beryllium oxide, deposited on aluminum 6101-T6 in contact with uncoated aluminum A356-T61. Titanium nitride coatings were deposited on copper C11000-H03 and aluminum 6101-T6 by PVD from a solid sputtering target between coating thicknesses of 1–5.5 μm. The thermal contact conductance values varied from 225 to 29754 W/m^2-K (38.6 to 5058.2 Btu/h ft^2 °F) for the range of parameters tested and showed a four times improvement over a nickel-plated coating, which is presently being employed.

Refractory ceramics, including silicon nitride, boron nitride, and aluminum nitride, were also deposited by PVD onto aluminum 6101-T6 from a sputtered solid target with coating thicknesses between 1–5 μm. The thermal contact conductance values for the three coating types ranged from 200 to 15,000 W/m^2-K (34.0 to 2550.0 Btu/h ft^2 °F) for the range of thicknesses, pressures, and temperatures tested. All three coating types showed two orders of magnitude improvement in thermal contact conductance as compared to an anodized coating that is presently being employed on aluminum 6101-T6.

The beryllium oxide coating was also deposited by PVD onto aluminum 6101-T6 from a solid target with coating thicknesses between 1–5 μm. The thermal contact conductance values ranged from 1308 to 24,000 W/m^2-K (230.36 to 4226.80 Btu/h ft^2 °F) for the range of parameters tested. A substantial decrease in thermal conductance for the 5-μm coating thickness was observed, but this can be attributed to the increase of the specimen out of flatness by a factor of 3 when compared to the other two specimens.

A comparison of the four individual ceramic coatings deposited on aluminum 6101-T6 in contact with uncoated aluminum A356-T6 clearly indicates that titanium nitride coatings have the highest thermal contact conductance for the entire thickness range investigated. The difference in thermal contact conductance values between the ceramic coatings becomes significant at pressures greater than 344 kPa (50 psi) when compared to a bare aluminum 6101-T6 to aluminum A356-T6 junction. Thus, as a replacement for anodization coatings that are presently being employed for most aluminum protection, titanium nitride is a suitable ceramic coating that will improve thermal contact conductance and also maintain the protective properties required for different environmental conditions. Beryllium oxide is also a suitable replacement for the anodization coatings, which also showed good thermal contact conductance values when compared to the anodized coating.

A thermomechanical model developed by Antonetti and Yovanovich was employed to determine predictability of thermal contact conductance values for the ceramic coatings types used in the investigation. The model curve lies well above the experimental values obtained for the bare surfaces, however, this is mainly due to the nonflat conditions employed for the specimens measured. The model curve also lies above the experimental values for several ceramic coatings, except for titanium nitride and beryllium oxide deposited on aluminum 6101-T6, however, a significant difference is observed between the predictive curve and experimental values at lower relative pressures for TiN and BeO coatings. The main causes of the deviation from the model may be the nonflat contacting surfaces and the lack of precise values for the thermal conductivities of the deposited coatings.

The thermal contact conductance values for the ceramic and oxide coatings measured in this study are also compared to Yip's model. The predictive curve for each material type lies well below the measured values, which indicates lower thermal contact resistance for the range of relative pressures tested. In addition, the slope of the predictive curves remains relatively flat with decreasing relative pressures while the measured values have an increasing negative slope.

Overall, the thermomechanical model developed by Antonetti and Yovanovich had greater success at predicting the general trend of the experimental data.

References

[1]Fletcher, L. S., "A Review of Thermal Enhancement Techniques for Electronic Systems," *IEEE Transactions on Components, Hy-*

brids, and Manufacturing Technology, Vol. 13, No. 4, 1990, pp. 1012–1021.

[2]Marotta, E. E., Lambert, M. A., and Fletcher, L. S., "A Review of the Thermal Contact Conductance of Non-Metallic Coatings and Films," *Journal of Thermophysics and Heat Transfer*, Vol. 8, No. 2, 1994, pp. 349–357.

[3]Majumdar, A., "Effect of Surface Deformations on Thermal Contact Conductance," *Proceedings of the NSF/DITAC Workshop on Thermal Conduction Enhancement in Microelectronics*, edited by A. Williams, Monash Univ., Melbourne, Australia, 1992, pp. 59–69.

[4]Fletcher, L. S., and Sparks, T. H., "Thermal Contact Conductance of Porous Ceramic Materials," *Proceedings of the NSF/DITAC Workshop on Thermal Conduction Enhancement in Microelectronics*, edited by A. Williams, Monash Univ., Melbourne, Australia, 1992, pp. 71–77.

[5]Sheffield, J. W., and Chung, K. L., "Thermal Contact Conductance of Metal-to-Metal and Metal-to-Ceramic Joints Within Microelectronic Packages," *Proceedings of the NSF/DITAC Workshop on Thermal Conduction Enhancement in Microelectronics*, edited by A. Williams, Monash Univ., Melbourne, Australia, 1992, pp. 13–18.

[6]Peterson, G. P., and Fletcher, L. S., "Measurement of the Thermal Contact Conductance and Thermal Conductivity of Anodized Aluminum Coatings," *Journal of Heat Transfer*, Vol. 112, No. 3, 1990, pp. 579–585.

[7]Lambert, M. A., and Fletcher, L. S., "Metallic Coatings for Enhancing the Thermal Contact Conductance of Electronic Modules," *Journal of Thermophysics and Heat Transfer*, Vol. 8, No. 2, 1994, pp. 341–348.

[8]Fletcher, L. S., Blanchard, D. G., and Kinnear, K. P., "Thermal Conductance of Multilayered Metallic Sheets," *Journal of Thermophysics and Heat Transfer*, Vol. 7, No. 1, 1993, pp. 120–126.

[9]Marotta, E. E., Blanchard, D. G., and Fletcher, L. S., "The Thermal Contact Conductance of Diamond-Like Films," AIAA Paper 93-0845, Jan. 1993.

[10]Kline, S. J., and F. A. McClintock, "Describing Uncertainties in Single-Sample Experiments," *Mechanical Engineering*, Vol. 75, No. 1, 1953, pp. 3–8.

[11]Lambert, M. A., Marotta, E. E., and Fletcher, L. S., "The Thermal Contact Conductance of Hard and Soft Coat Anodized Aluminum," *Journal of Heat Transfer*, Vol. 117, No. 2, 1995, pp. 532–537.

[12]Lambert, M. A., Marotta, E. E., and Fletcher, L. S., "Thermal Enhancement Techniques for SEM Guide Ribs and Card Rails, 1991 Annual Report," Conduction Heat Transfer Lab., Dept. of Mechanical Engineering, Texas A&M Univ., Rept. CHTL-6770-6, College Station, TX, Jan. 1992.

[13]Antonetti, V. W., and Yovanovich, M. M., "Enhancement of Thermal Contact Conductance by Metallic Coatings: Theory and Experiment," *Journal of Heat Transfer*, Vol. 107, Aug. 1985, pp. 513–519.

[14]Yip, F. C., "Effect of Oxide Films on Thermal Contact Resistance," AIAA Paper 74-693, July 1974.